Estimating surface soil moisture from TerraSAR-X data over two small catchments in Sahelian part of western Niger

N. Baghdadi, P. Camus, N. Beaugendre, O. Malam Issa, M. Zribi,
Jean-François Desprats, J.L. Rajot, C. Abdallah, C. Sannier

HAL Id: hal-00623114

https://hal.archives-ouvertes.fr/hal-00623114

Submitted on 13 Sep 2011

1 *Remote Sens.* **2011**, *3*, x-x manuscripts; doi:xx

6 *Article*

Estimating Surface Soil Moisture from TerraSAR-X Data over Two Small Catchments in Sahelian Part of Western Niger

9 **Nicolas Baghdadi [1,*], Pauline Camus [1], Nicolas Beaugendre [2], Oumarou Malam Issa [3,6], Mehrez**
10 **Zribi [4], Jean François Desprats [5], Jean Louis Rajot [6], Chadi Abdallah [7], Christophe Sannier [2]**

11 [1] CEMAGREF, UMR TETIS, 500 rue François Breton, 34093 Montpellier cedex 5, France
12 [2] SIRS, Villeneuve d'Ascq, France
13 [3] Université de Reims Champagne Ardenne, GEGENA EA 3795, France
14 [4] CESBIO, 31401 Toulouse, France
15 [5] BRGM, RNSC, 34000 Montpellier, France
16 [6] IRD, BIOEMCO, Niamey, Niger
17 [7] Lebanese National Council For Scientific Research, Remote Sensing Centre, Beirut, Lebanon

18 * Author to whom correspondence should be addressed; E-Mail: nicolas.baghdadi@teledetection.fr;
19 Tel.: +33-467548724; Fax: +33-467548700.

22

23 **Abstract:** The objective of this study is to validate an approach based on the change
24 detection in multitemporal TerraSAR images (X-band) for mapping soil moisture in
25 Sahelian area. In situ measurements were carried out simultaneously with TerraSAR-X
26 acquisitions on two study sites in Niger. The results show the need for using the difference
27 between the rainy season image and one reference image acquired in dry season. The use
28 of two images allows reducing the roughness effects. The soils of plateaus covered with
29 erosion crusts are dry throughout the year while the fallows show more important moisture
30 during the rainy season. The accuracy on the estimate of soil moisture is about 2.3%
31 (RMSE) in comparison with in situ moisture contents.

33

34 **1. Introduction**

1   Biological soil crusts are organo-mineral complexes resulting from the colonisation of the soil
2   surface by communities of micro-organisms, i.e. cyanobacteria, bacteria, algae, lichens and mosses.
3   They are widespread in arid and semi-arid environments where they performed a number of important
4   functions [1-6]. The ability of these organisms to colonize bare substrates is due to their ability to
5   withstand high temperatures, radiation, low water potential, their capability to move up, and down the
6   soil surface as a response to changes in soil moisture availability [7]. They also have the ability to
7   remain dormant at a dry state for long periods of time.

8   Within the Sahelian zone biological soil crusts (BSC) occurred associated with various types of
9   physical soil crusts in sandy soils left fallow and in soils of "tiger bush ecosystem" (landscape with a
10   typical pattern consisting of alternating densely vegetated bands comprising small trees and shrubs and
11   bare soil bands [5,8,9]. Their appearance at the soil surface was interpreted as the first sign of soil
12   degradation [10,11]. Their beneficial impact on ecological processes was observed on well-developed
13   type on degraded soil of Sahel in Western Niger [5,9,12,13]. Undisturbed BSCs enhance the quality of
14   degraded soil by providing a more stable structure and water retaining substratum [5,9,12] and
15   increasing fertility by N and C fixations [13].

16   Monitoring the location, extension and/or degradation of BSC is worth studying in order to evaluate
17   ecological functions of such crusts at regional scale. This study is a part of the BioCrust project
18   (Biological soil crusts vulnerability and soil surface disturbance in Sahelian zone), a project on
19   microbiotic crust vulnerability and soil degradation in Sahelian zone. The purpose of BioCrust is to
20   improve understanding of the temporal and spatial dynamics of BSCs in Sahelian ecosystems and to
21   provide tools for management in assessing soil degradation due to future changes in land uses and
22   climate.

23   The direct mapping of biological soil crusts from satellite imagery is not possible in Sahelian areas.
24   The mapping by optical imagery should determine the areas of potential presence and development of
25   biological crusts, based on favourable criteria to their development (in particular on the land
26   occupation such as fallow and plateaus). Moreover, as the presence and the development of biological
27   crusts is supposed dependent of soil moisture content, a relationship between radar signal and crusts
28   presence could be possible. Indeed, the radar signal is strongly depend on the soil moisture and it
29   seems that the biological crusts need certain moisture level for its development. With the radar
30   imagery, the soil moisture maps could be used to add supplementary information in the research of
31   favourable areas to crusts development.

32   Radar sensors allow mapping irrespective of meteorological conditions (clouds, fog, etc.), both day
33   and night. This is not the case with optical sensors, which are not possible if there is cloud cover, a
34   frequent situation in rainy season. The Soil Surface Characteristics can be estimated from microwave
35   remote sensing sensors due to the sensitivity of radar signal to soil characteristics such as the soil's
36   roughness and dielectric constant [14-16]. In addition, the radar signal depends on various radar
37   parameters such as the polarization, incidence angle and frequency. The penetration depth of radar
38   wave in vegetable cover is more important at high than at low radar wavelength (L-band
39   comparatively to X-band) [16]. Baghdadi et al. [17] showed in using TerraSAR-X data that after strong
40   rains the soil contribution to the backscattering of sugarcane fields can be important for canes with
41   heights less than 30cm. Thus, only bare soils or soils covered by a thin herbaceous layer could be used
42   for estimating soil moisture content.

1   The study concerns two study sites in Niger where Synthetic Aperture Radar (SAR) images of
2   TerraSAR-X sensor where acquired simultaneously to ground measurements. These results will
3   contribute to the implementation of a soil degradation and biocrust vulnerability monitoring tool. The
4   possibility of retrieving these soil parameters was widely investigated from C-band Synthetic Aperture
5   Radar [18-22]. A radar configuration that minimizes the effects of surface roughness is recommended
6   for a better estimate of soil moisture when using only one incidence angle. The optimal radar
7   incidences in C-band for the retrieval of soil moisture are weaker than 35° [21]. However, the use of
8   only one image is limited only to study areas with homogeneous values of surface roughness. The use
9   of two images acquired at two different incidence angles (low and high) allows the precision on the
10   estimated moisture to be markedly improved because both surface roughness and soil moisture could
11   be estimated [18,19,21]. This configuration is not possible with current SAR sensors. Indeed, the time
12   separating two SAR images acquired at two different incidences is several days, which limits the use
13   of this inversion procedure. Another solution involves the use of two SAR images, one in dry season
14   and one in rainy season. This method is easily applicable in Sahelian region where the soil roughness
15   remains unchanged except for cultivated areas. Moreover, the soil moisture in dry season could be
16   supposed equal to zero [22]. Many studies showed that with SAR imagery it is possible to estimate the
17   soil moisture with accuracy from 2 to 6% (RMSE) [19,21,22].

18   The objective of this study is to examine the potential of TerraSAR-X data for retrieving volumetric
19   soil moisture over Sahelian areas. This work evaluates if the use of two SAR images at X-band (one
20   reference image "dry season" and one image of interest "rainy season") improves the accuracy on the
21   estimate of surface soil moisture in comparison to only one image (without reference image). In
22   section 2, the study sites, the database including satellite images and experimental measurements are
23   described. Section 3 presents the proposed methodology for retrieval soil moisture. Finally,
24   conclusions and perspectives are presented in Section 4.

25   **2. Study sites and database**

26   *2.1. Study sites description*

27   Two study sites were chosen in the south-west part of Niger: Banizoumbou (13,53°N ; 2,67°E) and
28   Tamou (12,80°N ; 2,14°E) (Figure 1). The climate is semi arid with a rainy season between June and
29   October and an annual rainfall ranges from 140 mm in the North to 720 mm in the South with a
30   pluviometric gradient of 1 mm/km for the whole of western Niger. Average rainfalls of 500 mm and
31   650 mm are observed for Banizoumbou and Tamou, respectively [23]. The landscape is composed of
32   two major geomorphic units [24,25]:
33   (1) Plateaus formed by Tertiary fluvio-lacustrine deposits, capped by a thick laterite cuirass with
34   slight slopes of a maximum of one percent. They are dissected into several sections by erosion and
35   covered with tiger bush (*brousse tigrée*) or gapped bush (*brousse tachetée*) depending on the
36   alternation of bare soil and small trees that formed the bush [26]. The bush corresponds to tiger bush
37   (Figure 2a) when the bare soil and trees form long arcs or bands. The tiger bush pattern consists of
38   alternating lines of small trees about 4 m high and strips of bare or sparsely vegetated ground [27,28]
39   (Figure 2a). The distance between successive vegetated bands varies between 60 and 120 meters.
40   When the vegetation is not structured any more in bands but in gaps, bush is called gapped (Figure 2b).

1   2b). The mean distance between two consecutive gaps is about 50 meters for gapped bush. The bare
2   soil of plateaus is characterized by an important crusting due to strong precipitations in the rainy
3   season which runs off the surface. Water infiltrates in the vegetated bands and thus plays an important
4   role in the maintenance of these vegetated areas [29]. Three main classes are identified on plateau:
5   bare soil (with gravel), sparse vegetation, and dense vegetation.

6   (2) Sand dunes correspond to a transitional geomorphic unit between plateaus and the valleys
7   systems. They are formed by Pleistocene stabilised-sand with a mean slope of approximately 2 to 5%.
8   These are used for cropping pearl millet and cowpea, and support vegetation areas used for pasture
9   during fallow periods.

10   (3) Valleys systems, formed by Aeolian and colluvial sands, comprise broad sand plains or sand-
11   filled stream beds with a mean slope of three to five percent. The vegetation in the valleys is
12   dominated by cultivated fields (mainly millet) and fallow land. Fallows are temporarily not cultivated.
13   They contribute to the regeneration of soil. Old fallows contain relatively dense woody coverage while
14   recent fallows are covered by an herbaceous with sparse small trees.

15   **Figure 1.** Location of Banizoumbou and Tamou study sites in Niger.

16

17   The soil moisture measurements described below were performed along a transect from the plateaus
18   to the valley systems. The sites of measurements are located on fallow lands and bare areas of the
19   plateau where soil surface is characterised by the presence biological and physical soil crusts. No
20   measurements were performed among the vegetated areas of the plateaus.

1   **Figure 2.** Tiger bush (*Brousse tigrée*) plateau in Banizoumbou (a), Gapped bush plateau
2   in Tamou (b), view of biological crusts on lateritic soil of plateaux (c), view of biological
3   crusts on sandy soil of valley (d). In (a) and (b), vegetation appears in dark while lighter
4   pixels represent bare soil (optical images).

5
6   **(a)**   **(b)**

7
8   **(c)**   **(d)**
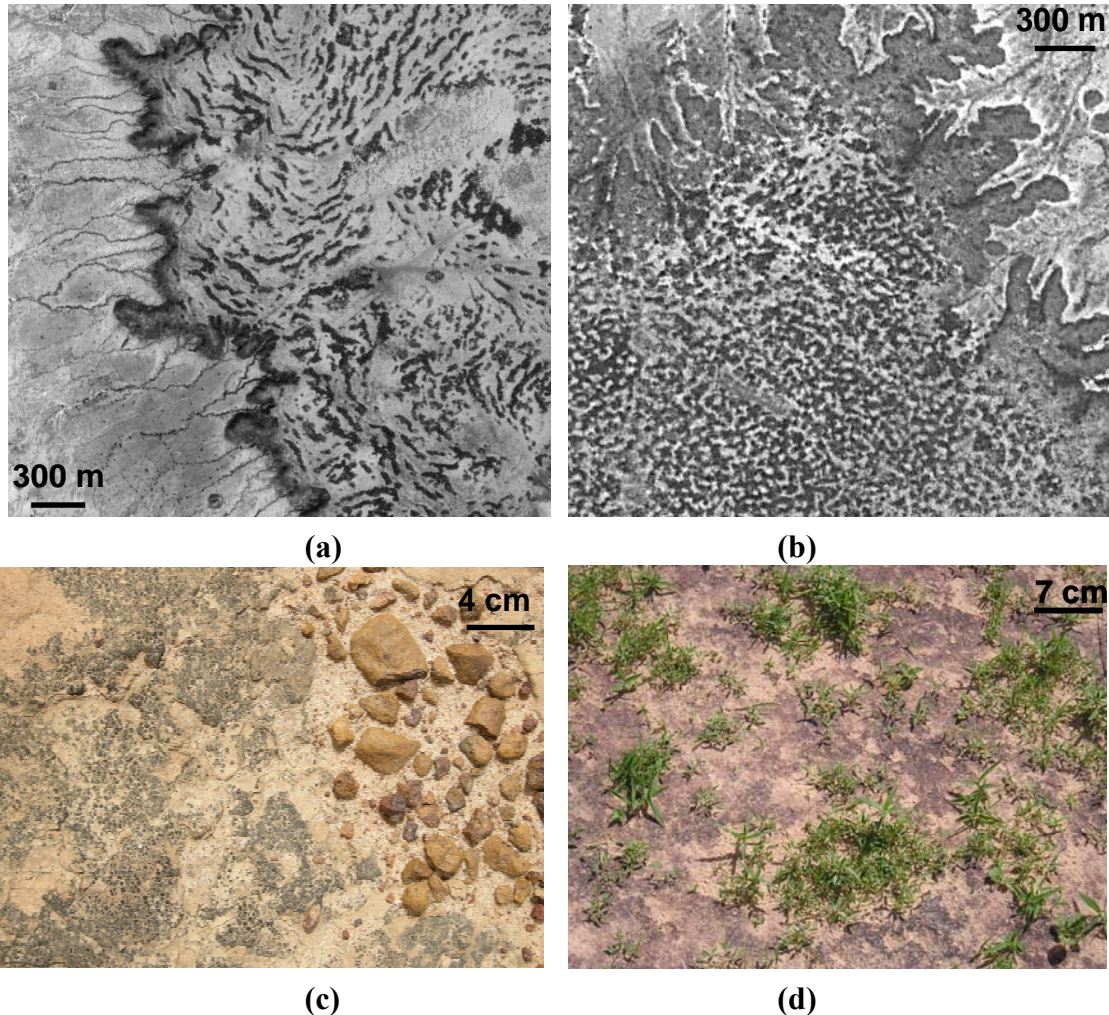
9   *2.2. TerraSAR images*

10   Fifteen TerraSAR-X images (X-band ~ 9.65 GHz) were acquired between the 29th of May and the
11   30th of October 2009 with incidence angles of 27° for Banizoumbou site and 39° for Tamou site. All
12   images were acquired in HH polarization and in Spotlight imaging mode (pixel spacing of 1m).
13   Characteristics of TerraSAR images used in this study are summarized in Table 1. Examples of
14   TerraSAR images are presented in Figure 3.
15   Radiometric calibration using MGD (Multi Look Ground Range Detected) TerraSAR images was
16   carried out using the following equation [30]:

$$\sigma^{\circ}_i (dB) = 10\log_{10}\left(Ks\,DN_i{}^2 - NEBN\right) + 10\log_{10}(\sin\theta_i) \qquad (1)$$

17   This equation transforms the amplitude of backscattered signal for each pixel (DN_i) into a
18   backscattering coefficient (σ°_i) in decibels. The calibration coefficient *Ks* (scaling gain value)
19   depends on radar incidence angle (θ_i) and polarization. It is given in the section "calibration" of the

1   TerraSAR data delivery package. NEBN is the Noise Equivalent Beta Naught. It represents the
2   influence of different noise contributions to the SAR signal. The NEBN is described using a
3   polynomial scaled with *Ks*. The polynomial coefficients are derived from the TerraSAR product file
4   (section "noise" of SAR data delivery package). The absolute radiometric accuracy of TerraSAR data
5   is better than 0.6 dB [30]. All TerraSAR images were then georeferenced using GPS points (cubic
6   convolution resampling algorithm). The RMS georeferencing accuracy varies from 1.5 to 1.9 pixels.

7   **Table 1.** List of TerraSAR-X images. Universel time (TU) = Local time - 1 hour.

Study site	Acquisition date	Acquisition hour (TU)	Season
Banizoumbou	29 May 2009	17h51	Dry
	01 July 2009		
	23 July 2009		Rainy
	14 August 2009		
	25 August 2009		
	16 September 2009		
	08 October 2009		
	30 October 2009		
Tamou	04 June 2009	05h44	Dry
	07 July 2009		
	29 July 2009		Rainy
	31 August 2009		
	11 September 2009		
	22 September 2009		
	14 October 2009		

8   **Figure 3.** TerraSAR images on Banizoumbou and Tamou. The size of each study site is 10
9   km x 10 km.
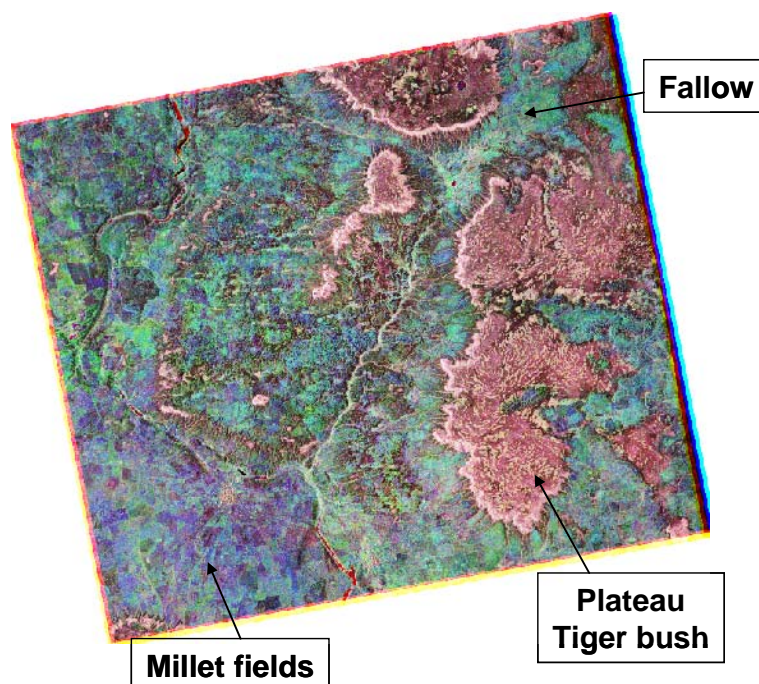
10
11   *Banizoumbou, RGB= 29 May, 14 August and 08 October 2009*

1   **Figure 3.** *Cont.*
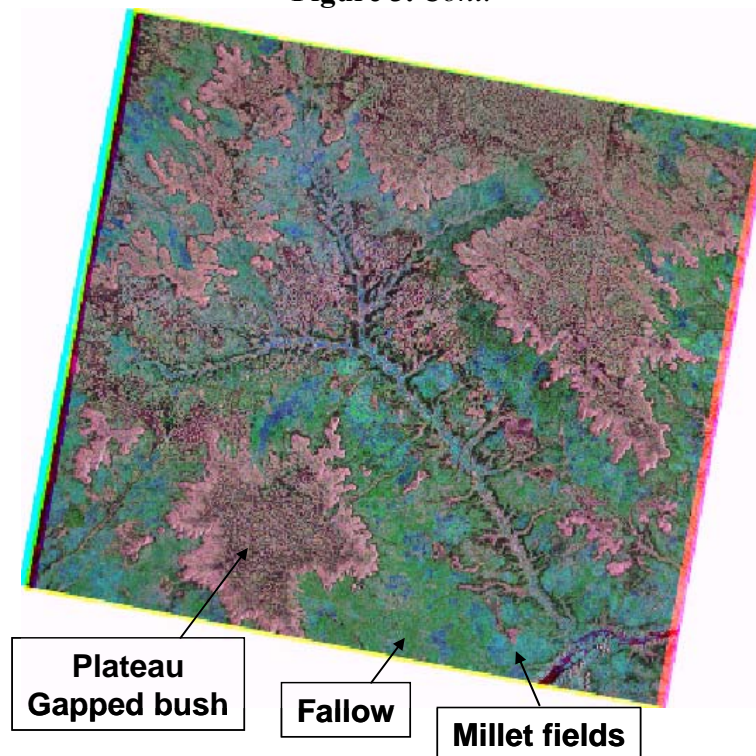
Tamou, RGB=04 June, 29 July and 14 October 2009

Speckle noise, due to the coherent interference of waves reflected from many elementary scatterers, is present on SAR images and makes the pixel-by-pixel interpretation of TerraSAR images extremely difficult. This explains why the analysis of radar signals is generally carried out on homogeneous areas with several pixels or at field scale (which helps reduce speckle). In practice, the mean backscattering coefficients are calculated from calibrated TerraSAR images by averaging the linear $\sigma°$ values of all pixels within reference fields or over cells of N pixels (kernels of N pixels).

2.3. Optical images

Very high spatial resolution optical images were also collected on Banizoumbou (July and September 2009) and Tamou (June, August, September, and November 2009) from Kompsat-2 sensor (http://www.kari.re.kr/eng/). Images have spatial resolutions of 1 m in panchromatic mode and 4 m in multispectral mode (blue, green, red, infrared). These images were used to allow a reliable mapping of land surface types: water, forest thickets (*fourré),* fallow, cultivated fields, bare soil mainly in fallow, bare stony soil mainly on plateau, and village (Figure 4). The class forest thicket represents mainly the vegetation situated on plateaus. The detailed land use maps were produced by Computer Assisted Photo-Interpretation (CAPI). The analysis of diachronic images between dry and rainy seasons was particularly useful for differentiating land use, and more especially bare soil and cultivated area. CAPI was preferred to other classification techniques because the information contained in the Kompsat imagery was used to its maximum.

The estimation of soil moisture will be realized only on bare soils or soil with thin herbaceous layer. The Normalized Difference Vegetation Index (NDVI) was computed from the optical image in the red and infrared bands (NIR-Red/NIR+Red), and NDVI values under an empirical threshold of 0.25 were

1 found using photo interpretation for mapping bare soils and thin herbaceous areas. The bare soil
2 (herbaceous areas of fallows and laterite cuirass soils without vegetation of plateaus) represents
3 approximately 36% of Banizoumbou study site and 41% of Tamou site. As the development of BSCs
4 requires the absence of tillage and trampling, the cultivated areas were excluded of the soil moisture
5 mapping.

6   **Figure 4.** Illustration of landuse/landcover conditions in 2009 on Banizoumbou (on a
7   segment of Kompsat image).
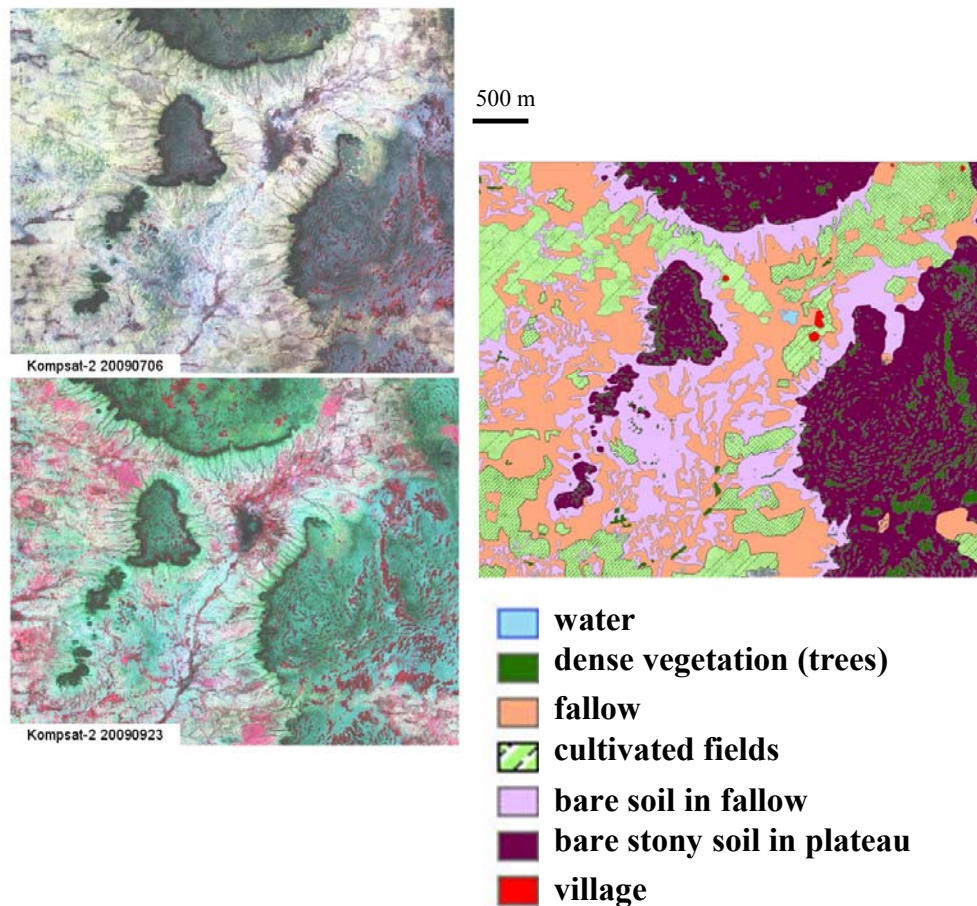
8
9 *2.4. Soil Moisture Measurements*

10   Simultaneously to TerraSAR acquisitions, in situ measurements of volumetric soil moisture have
11 been carried out on the first top 5 cm using 5-cm-long vertically installed TDR probe (Time Domain
12 Reflectometry). The radar signal penetration depth is only of few centimetres at X-band [16]. The soil
13 moisture content ranges from 0% to 21.5% (Table 2), with single-field standard deviation between 0.5
14 and 2%. Due to high evaporation rates, only in situ measurements collected within a time window of 2
15 hours will be used. However, the logistic difficulties, in particular ease of access to study site and the
16 absence of support facilities, did not allow collecting in situ soil moisture measurements
17 simultaneously to each radar acquisition.
18   Six to twenty one training areas were chosen for each ground campaign. The volumetric water
19 content on a training area scale is assumed to be equal to the mean value of five to eight soil moisture
20 measurements collected on the training area. The surface of our training areas is variable but the

1   minimal size is of approximately 100m². In situ observations show that the laterite soils of plateaus,
2   covered with erosion crusts, have soil moistures nulls.
3
4   **Table 2.** Characteristics of in situ measurements mainly on fallows. The soil moisture
5   content on plateaus is null.

Site	TerraSAR images (2009)		Ground measurements (2009)				
	Date	Acquisition Time (TU)	Date	Time (TU)	Training areas	Soil moisture content (%)	Comment
Banizoumbou	29 May	17h51	-	-	-	<1	-
	01 July	17h51	-	-	7	<1	Rainfall rate = 7mm from 2h20 AM to 5h50 AM
	23 July	17h51	23 July	10h30-11h30	21	0 – 5.3	In situ measurements seven hours before SAR acquisition
	14 August	17h51	14 August	17h15-18h30	9	7.4 – 10.7	-
	25 August	17h51	25 August	17h30-19h00	11	4.1 – 9.6	-
	16 September	17h51	16 September	17h40-18h40	9	2.7 – 5.4	-
	08 October	17h51	08 October	17h35-18h35	10	0 – 3.8	-
	30 October	17h51	30 October	17h35-18h35	11	1.7 – 3.7%	-
Tamou	04 June	05h44	-	-	-	<1	-
	07 July	05h44	07 July	4h30-5h45	6	3 – 3.1	Rainfall rate = 18mm from 23h25 to 23h59
	29 July	05h44	30 July	5h10-6h35	14	9.4 – 12.6	-
	31 August	05h44	01 September	5h25-6h45	13	16.9 – 21.5	Rainfall rate = 49mm from 9h13 AM on August 31 to 2h35 AM on September 01 Data not exploitable
	11 September	05h44	-	-	-	-	Rainfall rate = 1mm from 1h51 AM to 2h36 AM
	22 September	05h44	23 September	5h20-6h30	9	5.2 - 9.8	-
	14 October	05h44	14 October	5h30-6h40	7	0 – 3.2	-

6   The soil moisture content measurements on Banizoumbou were carried with less than one hour of
7   TerraSAR acquisitions, except for the image acquired on July 23 where seven hours separate in situ
8   measurements from SAR acquisition (Table 2) (measurements not used). On the Tamou site, some
9   ground campaigns were carried out at one day of TerraSAR acquisitions. Thus, only data acquired

1   simultaneously to SAR acquisitions (± 2 hours) would be used in the definition of relationship between
2   backscattering coefficient and soil moisture.
3   Climatological data were available from the nearest meteorological station including daily mean
4   temperature for Banizoumbou site and rainfall rates for both Banizoumbou and Tamou sites. The
5   meteorological station used for Banizoumbou is located in the square of TerraSAR image whereas that
6   for Tamou is located 20km northeast of Tamou (at Dyabou) (Figure 5).

7   **Figure 5.** Meteorological data recorded close to the study site and in situ soil moisture
8   content for our training areas: Banizoumbou (a) and Tamou (b).
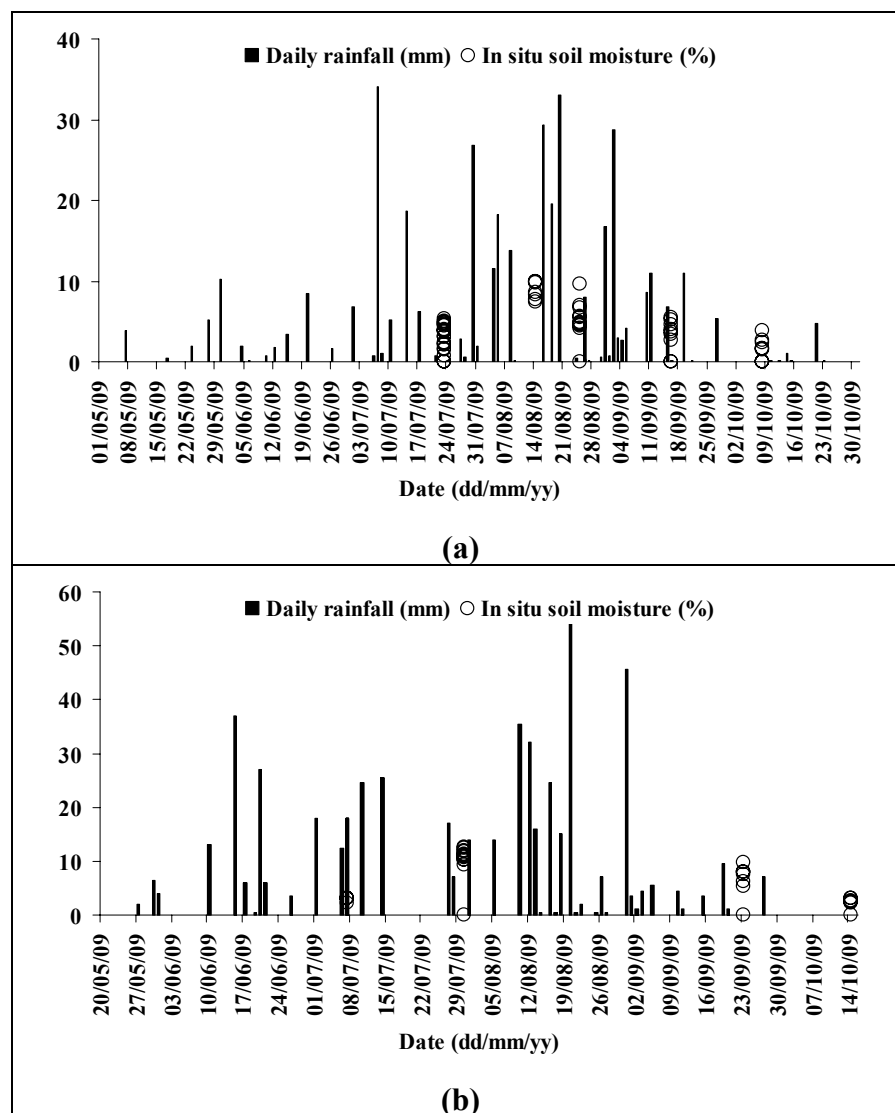
9   **3. Soil moisture mapping**

10   *3.1. Relationship between radar signal and soil moisture*

11   For bare soils, the radar backscattering coefficient in decibels can be written as the sum of two
12   functions, one linear to describe the dependence of radar signal on volumetric surface soil moisture
13   (for values between 5% and 35%), and one exponential to illustrate the dependence of $\sigma°$ on surface
14   roughness [16,18,21,31]:

$$\sigma_{dB}^0 = a\,m_v + b\,e^{-krms} + c \qquad (2)$$

1 where k is the wave number (≈ 2 cm^{-1} for X-band), and *rms* is the root mean square surface height
2 (surface roughness). For a given radar wavelength, the coefficients *a, b*, and *c* are observed to be
3 dependent on both radar incidence angle and polarization [19, 21, 31]. To retrieve soil moisture (m_v)
4 from a single radar configuration, it is necessary to establish a relationship between the radar
5 backscattering coefficient (σ°) and m_v alone, without having any knowledge of the *rms* surface height.
6 As a first approximation, the radar backscattering coefficient (in dB) may be expressed as follows
7 [16,21]:

$$\sigma_{dB}^0 = a\,m_v + d \qquad (3)$$

8 This simplified relationship ignores the surface roughness. The coefficient *a* is dependent on both
9 incidence angle and polarization. The coefficient *d* is primarily controlled by incidence angle,
10 polarization and surface roughness (for a given radar wavelength).

11 To eliminate the soil roughness effects, a reference image acquired in dry season could be used. The
12 difference between one image acquired during the rainy season (soil moisture = m_v) and the reference
13 image ($\Delta\sigma^\circ$) can be expressed as [22]:

$$\Delta\sigma_{dB}^\circ \approx a'\,m_v \qquad (4)$$

14 This approach assumes that the soil roughness is unchanged between the two SAR acquisition
15 dates. This condition is valuable for bare soils, except for cultivated fields. Moreover, the assumption
16 that the soil moisture in dry season is null is verified by ground measurements.

17 The development of biological crusts requires wet soil and little anthropic disturbance. Moreover,
18 their presence is limited mainly to fallows and plateaus. Thus the approaches for mapping soil
19 moisture as defined in equations (3) and (4) will be applied on bare soils and areas with short
20 herbaceous layer in using TerraSAR imagery. First, from a part of the database (25% of 91 points σ°
21 and m_v) the relationship defined in equation (3) between the radar backscattering coefficient and the in
22 situ soil moisture content was established. Indeed, a mean backscattering coefficient was calculated for
23 each soil moisture measurement in using pixels around the location of moisture content measurements
24 (on homogeneous area around GPS location).

25 However, TerraSAR images acquired on July 29, August 31 and September 22 had not been used in
26 the calibration phase of relationships between σ° and m_v (equations 3 and 4) because the associated
27 ground measurements of moisture content were carried out one day after acquisitions (Table 2).
28 Moreover, in the night of August 31, strong rains were recorded, making impossible the use of data of
29 August 31 and September 1. Finally, the SAR image on September 11 cannot be exploited for lack of
30 ground measurements.

31 The coefficients *a* and *d* of equation 3 were then calculated as a function of incidence angle,
32 regardless of soil roughness. Figure 6 shows the linear relationships between radar signal and soil
33 moisture for each study site. An offset between the two relationships about 1.3dB shows the effect of
34 radar incidence angle, with higher σ° for Banizoumbou images than for Tamou images (27° for
35 Banizoumbou and 39° for Tamou). Results show that the sensitivity of the radar signal to soil moisture
36 is of the same order for 27° and 39° (0.292 dB/% for 27° and 0.287dB/% for 39°. These results

1   therefore show that moisture mapping is optimal at low and medium <u>incidence angles</u>. In the case

2   where two TerraSAR images with the same incidence angle were used, one in dry season and one in

3   rainy season (equation (4)), the sensitivity of the difference $\Delta\sigma°$ (dB) to soil moisture is about 0.32

4   dB/% (Figure 7).

5   **Figure 6.** Sensitivity of TerraSAR-X signal to surface soil moisture for each study site

6   (27° for Banizoumbou and 39° for Tamou). Each point corresponds to the average

7   backscattering coefficient in decibels of pixels around in situ measurements of soil

8   moisture.
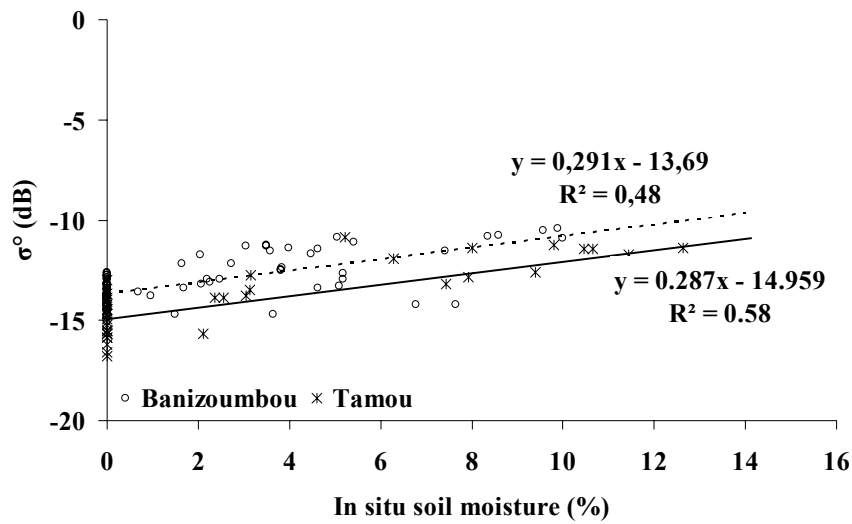
9

10   **Figure 7.** The difference between TerraSAR images acquired in rainy season and one

11   reference image acquired in dry season according to soil moisture.
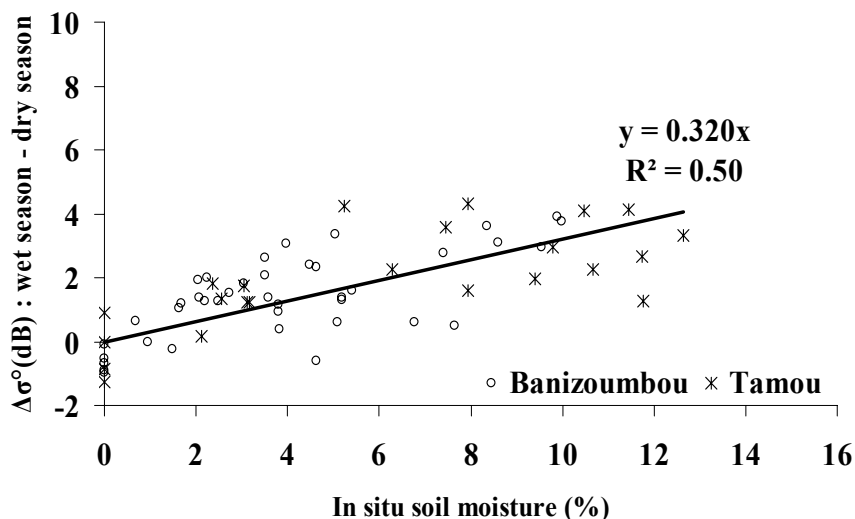
12

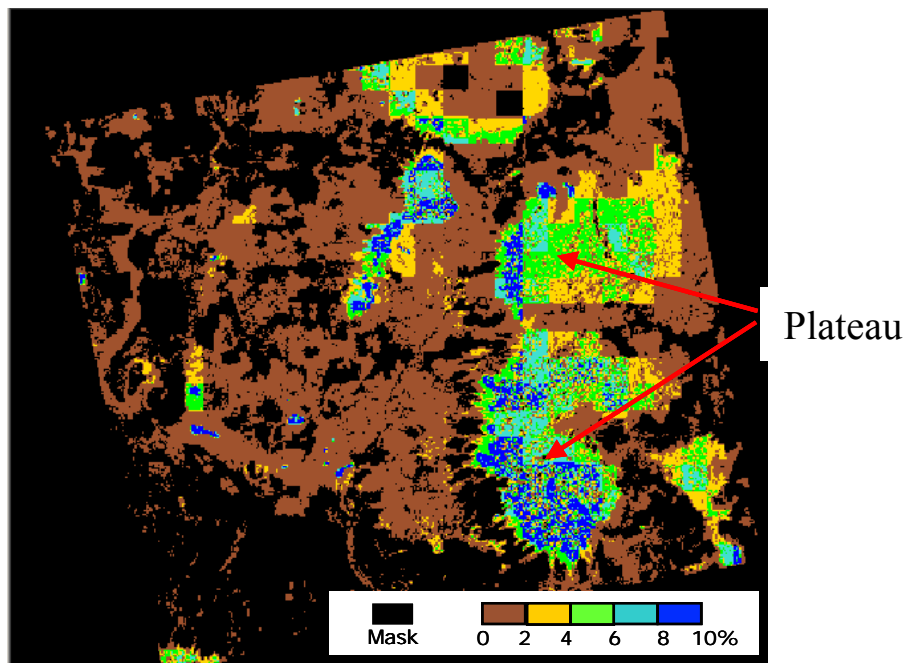13   *3.2. Soil moisture mapping*

14   Soil moisture estimates are obtained by inverting the relationships between radar signal and the soil

15   moisture (equations 3 and 4). The two simple procedures defined above were applied for mapping the

16   surface soil moisture. Only bare soils or soil with thin herbaceous layer (NDVI<0.25) were used for

17   soil moisture mapping. The study sites were divided into contiguous cells/areas of 500m x 500m

1   before calculating in each cell and for each land surface class the mean backscattering coefficient on

2   the whole of bare soil pixels belonging to each class. So, in each cell, we will have as many values of

3   mean σ° as of classes present in the cell. This approach for soil moisture mapping in each cell and for

4   each class is justified by the difference in the soil type of each class (different soil moisture levels).

5   <u>The soil moisture retrieval approach using radar images with a georeferencing accuracy of about 2</u>

6   <u>m (1.5 to 1.9 pixels) is compatible with optical images having a pixel spacing of 4 m (used to extract</u>

7   <u>the bare soils). Indeed, the georeferencing accuracy of radar images is smaller than the pixel spacing of</u>

8   <u>optical images. Moreover, the soil moisture mapping will be made in cells gathering several pixels.</u>

9   The in situ soil moisture in each cell and for each land surface class is assumed to be equal to the

10   mean value of all moisture measurements present in each cell. Validation of soil moisture retrieval

11   algorithm was carried in comparing in situ data and estimations derived from TerraSAR-X using the

12   inversion model (equations (3) and (4)). The use of a single TerraSAR image (method 1) overestimates

13   the moisture content on plateaus of about 6.3% (with RMSE=6.6%). This <u>over-estimation</u> of soil

14   moisture on plateaus is due to a stronger soil roughness (cuirass) whereas the soil of fallows is

15   relatively smoother (sandy). Moreover, the limit between low lands and plateaus appears also very

16   wet, that is related to important slopes at these areas. Figure 8 shows the soil moisture map on May 29

17   (dry season) over Banizoumbou. At this date, the estimated soil moisture is almost null on the whole of

18   the site except on the plateaus where strong erroneous values are observed (reach 8%).

19   **Figure 8.** Soil moisture mapping over Banizoumbou on May 29 by method 1 (cells of

20   500x500 pixels). The image covers 10 km x 10 km.

21

22   The mapping of soil moisture is much more coherent by using the difference between two images,

23   one acquired <u>in the dry season</u> (May 29 for Banizoumbou and June 04 for Tamou) and one <u>in the rainy</u>

24   <u>season</u> (method 2), since this difference eliminates the surface roughness effect. Figure 9 shows on the

25   estimated soil moisture map of August 25 (Banizoumbou) low soil moisture values on plateaus in

26   using method 2. Indeed, the estimated moisture on plateaus is close to 0 with method 2, which is closer

1   to the ground observations. Finally, the analysis of soil moisture temporal evolution during the year, on
2   Tamou for example (Figure 10), shows that moisture content remains stable on the plateaus (0-2%
3   over all the year) and it changes in low lands. Figure 11 and Table 3 show the comparison between
4   estimated and measured soil moistures. Method 1 overestimates the soil while method 2 provides
5   better results. The in situ moistures null correspond to strong values of estimated moistures (up to
6   11%) with the method 1 which neglects the effect of roughness. That relates mainly samples located on
7   the plateaus. With the method 2, these moistures are estimated at values close to 0. The mean
8   difference between estimated and measured soil moisture is lower than 1% with method 2 and about
9   3% with method 1. The resulting RMSE is about 2% with method 2 and 4% with method 1.

10   **Figure 9.** Result of soil moisture mapping in using methods 1 and 2 on August 25 (cells of
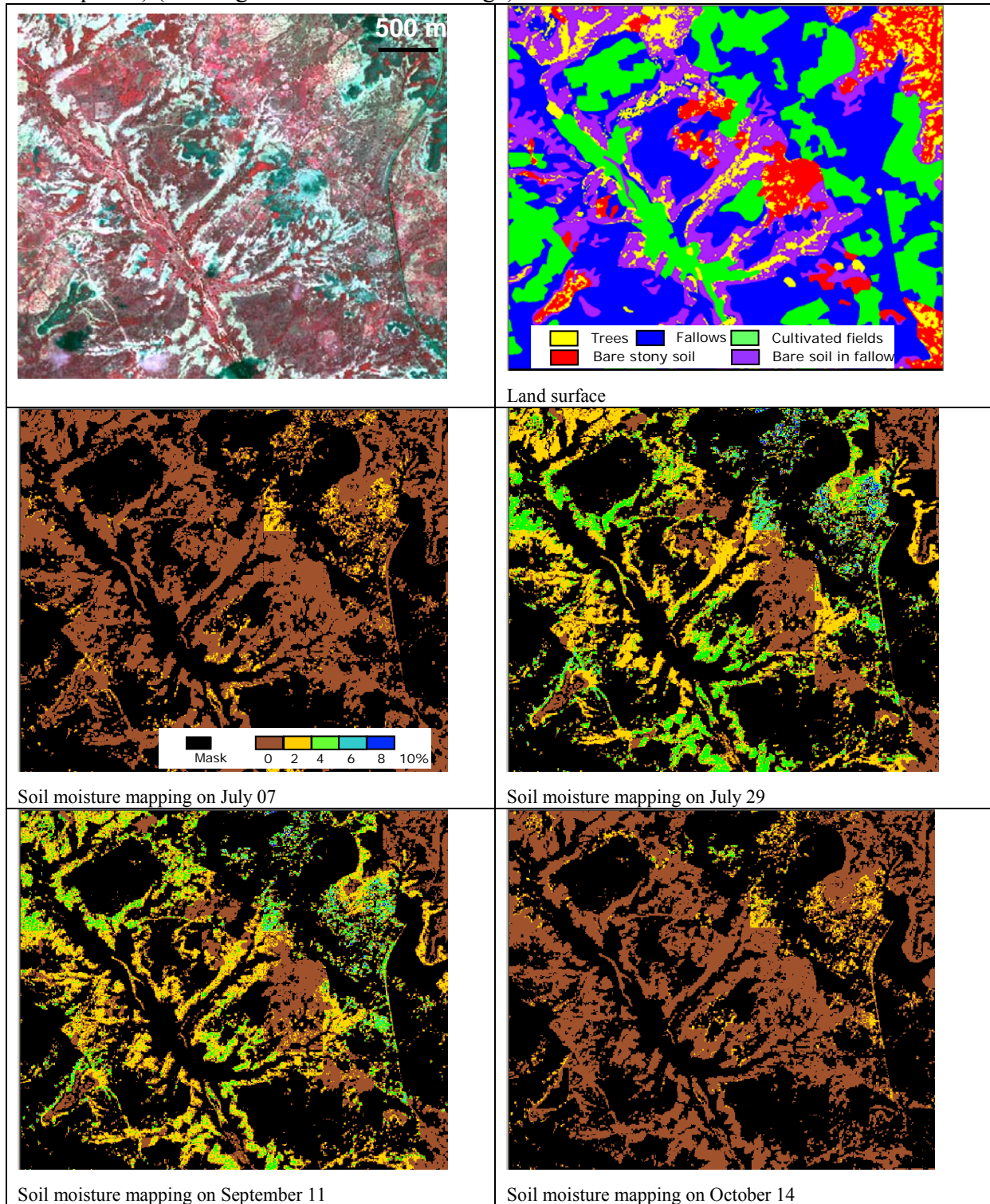11   500 x 500 pixels). The image covers 10 km x 10 km.

12
13   **Method 1**   **Method 2**
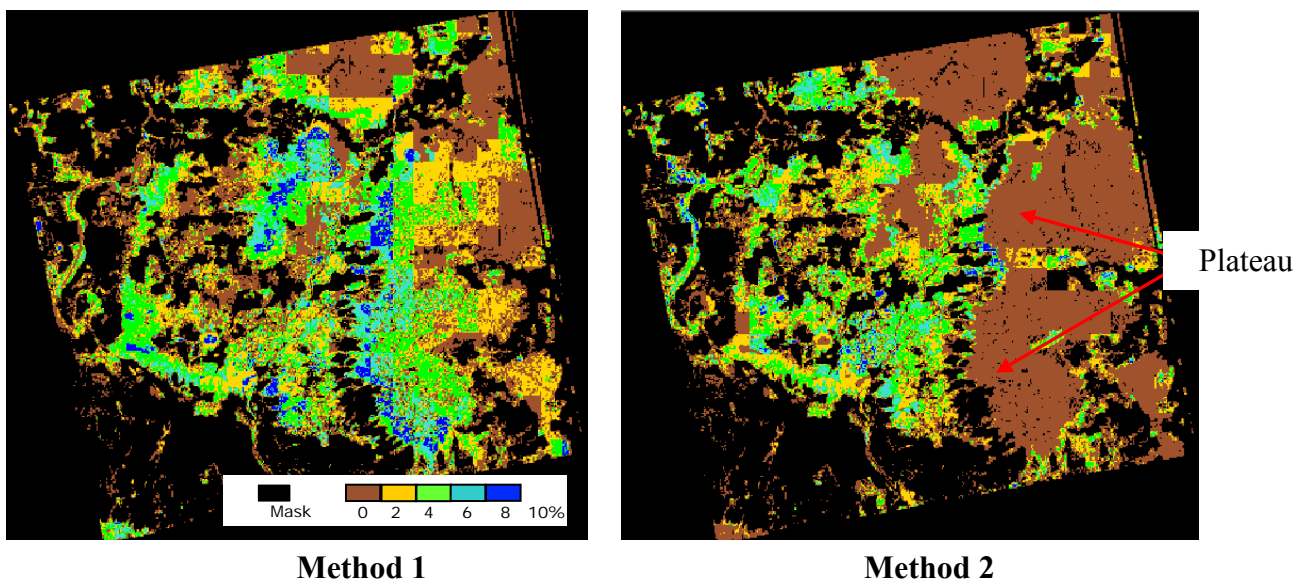
14   **4. Conclusions and perspectives**

15   The objective of this work was to propose a methodology for mapping soil moisture in semi arid
16   area (Sahel). Soil moisture maps were estimated on the two study sites of Banizoumbou and Tamou in
17   Niger. The results show the need for using two SAR images, one acquired in rainy season and one
18   acquired in dry season, in order to eliminate the roughness effects. Estimated soil moisture values are
19   almost null throughout the year on soils of plateaus covered with erosion crusts, but they change in the
20   low lands. Moreover, the bare soils of fallows show strong moisture contents throughout the rainy
21   season. Finally, soil moistures could be estimated with a RMSE of 2,3% in comparison with in situ
22   measurements.
23   In perspective, it would be necessary to use the soil moisture maps to analyze a possible correlation
24   between the soil moisture values and the presence of biological crusts. We could wonder whether high
25   moisture values in rain season will condition the development of crusts and if the presence of crusts is
26   limited to areas with low annual variations of moisture.
27
28

Figure 10. Temporal evolution of soil moisture map on Tamou (method 2, cells of 500 x 500 pixels) (on a segment of TerraSAR image).

Land surface

Soil moisture mapping on July 07

Soil moisture mapping on July 29

Soil moisture mapping on September 11

Soil moisture mapping on October 14

1   **Figure 11.** Comparison between estimated and in situ soil moisture contents. The over-
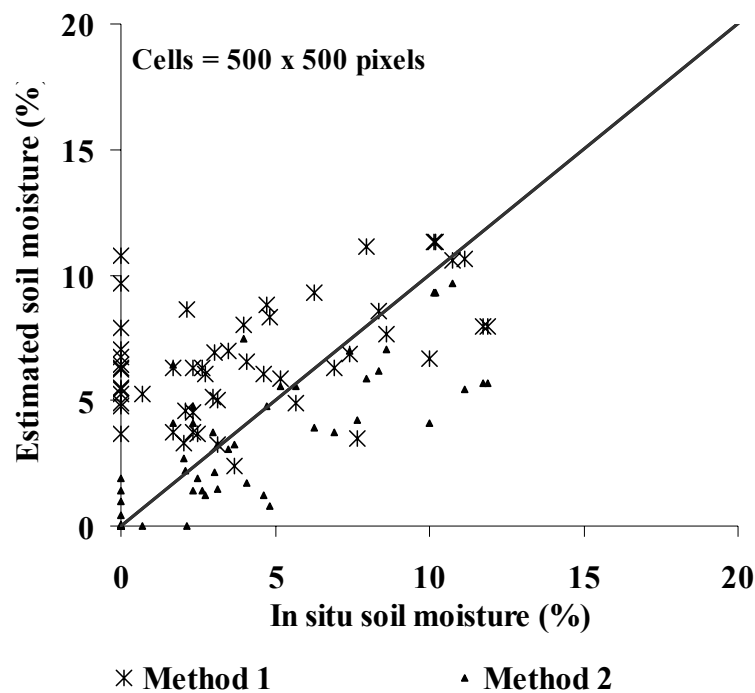2   estimate of soil moisture on plateaus (very low *mv*) is due to a stronger soil roughness
3   (cuirass).

4

5   **Table 3.** Analysis of differences between estimated and measured soil moisture. The test
6   with cells of 500x500 pixels use the land surface condition (in each cell, there are as many
7   moisture values as of land surface classes).

Method	1	2
Bias	+2,7	-0.8
Standard deviation	3,3	2,2
RMSE	4,2	2,3

8   **Acknowledgements**

14   **References**

15   1.   West, N.E. Structure and function of microphytic soil crusts in wildland ecosystems of arid to
16   semi-arid regions. *In: Advances in ecological research*, Academic Press, **1990**, 20, 179-222.
17   2.   Eldridge, D.J.; and Greene, R.S.B. Microbiotic soil crusts: a review of their role in soil and
18   ecological processes in the rangeland of Australia. *Australian Journal of Soil Research*, **1994**, 32,
19   389-415.

3. Verrecchia, E.; Yair, A.; Kidron, G.J.; and Verrecchia, K. Physical properties of the psammophile cryptogamic crust and their consequences to the water regime of sandy soils, north-western Negev desert, Israël. *Journal of Arid Environments*, **1995**, 29, 427–437.

4. Pérez, F.L. Microbiotic crusts in the high equatorial Andes, and their influence on 502 paramo soils. *Catena*, **1997**, 31, 173–198.

5. Malam Issa, O.; Tichet, J.; Défarge, C.; Couté, A.; and Valentin, C. Morphology and microstructure of microbiotic soil crusts on a tiger bush sequence (Niger, Sahel). *Catena*, **1999**, 37, 175-196.

6. Belnap, J. The potential roles of biological soil crusts in dryland hydrologic cycles. *Hydrological Processes*, **2006**, 20, 3159-3178.

7. Garcia-Pichel, F.; and Pringault, O. Cyanobacteria track water in desert soils. *Nature*, **2001**, 413, 380-381.

8. D'Herbes, J.M.; Valentin, C. Land surface conditions of the Niamey region, ecological and hydrological implications. *Journal of Hydrology*, **1997**, 188-189, 18-42.

9. Malam Issa, O.; Le Bissonnais, Y.; Défarge, C.; and Tichet, J. Role of a cyanobacterial cover on structural stability of sandy soils in Sahelian part of western Niger. *Geoderma*, **2001a**, 101, 15-31.

10. Dulieu, D.; Gaston, A.; and Darley, J. La dégradation des pâturages de la région de N'Djamena (République du Tchad) en relation avec la présence des cyanophycées psammophiles. Etude préliminaire. *Revue d'élevage et de medicine vétérinaire des pays tropicaux*, **1977**, 30, 181-190.

11. Hahn, A.; and Kusserow, H. Spatial and temporal distribution of algae in soil crusts in the Sahel of W Africa: Preliminary results. *Willdenowia*, **1988**, 28, 227-238.

12. Défarge, C.; Malam Issa, O.; and Trichet, J. Apports du Cryo-microscope électronique à balayage à émission de champ à l'étude des matières organiques et des relations organo-minérales naturelles. II. Application aux croûtes microbiotiques des sols. *Comptes Rendus Académie des Sciences*, **1999**, 328, 591-597.

13. Malam Issa, O.; Stal, L.J.; Défarge, C.; Trichet, J.; and Couté, A. Nitrogen fixation by microbial crusts from desiccated Sahelian soils (Niger). *Soil Biology Biochemistry*, **2001b**, 33, p. 1425-1428.

14. Dobson, M.C.; and Ulaby, F.T. Active microwave soil moisture research. *IEEE Transactions on Geoscience and Remote Sensing,*, **1986**, 24, 23–36.

15. Fung, A.K. Microwave scattering and emission models and their applications; Artech House, Inc., Boston, London, **1994**.

16. Ulaby, F.T.; Moore, R.K.; and Fung, A.K. Microwave Remote Sensing, Active and Passive, From Theory to Applications; Artech House, Inc.: Norwood, MA, USA, **1986**, Vol. 3.

17. Baghdadi, N.; Cresson, R.; Todoroff, P.; and Soizic, M. Multitemporal observations of sugarcane by TerraSAR-X images. *Sensors*, **2010**, 10(10), 8899-8919; doi:10.3390/s101008899.

18. Zribi, M.; and Dechambre, M. A new empirical model to retrieve soil moisture and roughness from C-band radar data. *Remote Sensing of Environment,* **2002**, 84, 42-52.

19. Srivastava, H.S.; Patel, P.; Manchanda, M.L.; and Adiga, S. Use of multi-incidence angle RADARSAT-1 SAR data to incorporate the effect of surface roughness in soil moisture estimation. *IEEE Transactions on Geoscience and Remote Sensing,* **2003**, 41 (7), 1638-1640.

20. Oh, Y. Quantitative retrieval of soil moisture content and surface roughness from multipolarized radar observations of bare soil surfaces. *IEEE Transactions on Geoscience and Remote Sensing,* **2004**, 42(3), 596-601.

21. Baghdadi, N.; Holah, N; and Zribi, M. Soil moisture estimation using multi-incidence and multi-polarization ASAR data. *International Journal of Remote Sensing*, **2006**, 27(10): 1907-1920.

22. Zribi, M.; Saux-Picart, S.; André, C.; Descroix, L.; Ottlé, C.; and Kallel, A. Soil moisture mapping based on ASAR/ENVISAT radar data over a Sahelian region. *International Journal of Remote Sensing*, **2007**, 28 (15-16), 3547-3565.

23. Le Barbé, L.; and Lebel, T. Rainfall climatology of the HAPEX-Sahel region during the years 1950-1990. *Journal of Hydrology*, **1997**, 188-189: 43-73.

24. Valentin, C. Effects of grazing and trampling on soil deterioration around recently drilled water-holes in the Sahelian zone. In: El Swaïfy, S.A., Moldenhauer, WL. and Lo A., ed., Soil erosion and conservation. Soil Conservation Society of America, Ankeny, **1985**, 51-65.

25. Courault, D.; D'Herbes, J.M; and Valentin, C. Le bassin versant de Sama Dey: premières observations pédologiques et phyto-écologiques, *ORSTOM edition*, Paris, **1990**.

26. Ambouta, J.M.K. Définition et caractérisation des structures de végétation contractée au Sahel: cas de la brousse tigrée nigérien. *JM d'Herbès , JM K. Ambouta, R. Peltier. John Libbey Eurotext,* Paris, **1997**, 41-57.

27. White, L.P. Brousse Tigree Patterns in Southern Niger. *Journal of Ecology*, **1970**, 58(2), 549-553.

28. Seghieri, J.; Galle, S.; Rajot, J.L.; and Ehrmann, M. Relationships between the soil moisture regime and the growth of the herbaceous plants in a natural vegetation mosaic in Niger. *Journal of Arid Environment*, **1997**, 36: 87–102

29. Galle, S.; Seghieri, J.; and Mounkaila, H. Fonctionnement et gestion des écosystèmes forestiers contractés sahéliens. *John Libbey Eurotext*. Chapitre 9, Fonctionnement hydrologique et biologique à l'échelle locale. Cas de la brousse tigrée au Niger, **1997**, 105-118.

30. Fritz, T.; and Eineder, M. TerraSAR-X Ground Segment Basic Product Specification Document (24.02.2008), Doc.: TX-GS-DD-3302, **2008**, Issue, 1.5, 103 pages, Available online: *http://www.acq.osd.mil/nsso/ais/texas_Docs/13-2%20TX-GS-DD-3302_Basic-Product-Specification-Document_1.5.pdf*

31. Holah, H.; Baghdadi, N.; Zribi, M.; Bruand, A.; and King, C. Potential of ASAR/ENVISAT for the characterisation of soil surface parameters over bare agricultural fields. *Remote Sensing of Environment*, **2005**, 96, 78-86.